

PCCP

Accepted Manuscript



This is an *Accepted Manuscript*, which has been through the Royal Society of Chemistry peer review process and has been accepted for publication.

Accepted Manuscripts are published online shortly after acceptance, before technical editing, formatting and proof reading. Using this free service, authors can make their results available to the community, in citable form, before we publish the edited article. We will replace this *Accepted Manuscript* with the edited and formatted *Advance Article* as soon as it is available.

You can find more information about *Accepted Manuscripts* in the [Information for Authors](#).

Please note that technical editing may introduce minor changes to the text and/or graphics, which may alter content. The journal's standard [Terms & Conditions](#) and the [Ethical guidelines](#) still apply. In no event shall the Royal Society of Chemistry be held responsible for any errors or omissions in this *Accepted Manuscript* or any consequences arising from the use of any information it contains.

ARTICLE

Aqueous Self-Assembly of a Charged BODIPY Amphiphile via Nucleation-Growth Mechanism†

Cite this: DOI: 10.1039/x0xx00000x

Le Yang,^a Gang Fan,^a Xiangkui Ren,^a Lingyun Zhao,^b Jinkang Wang^a and Zhijian Chen^{*a}Received 00th January 2012,
Accepted 00th January 2012

DOI: 10.1039/x0xx00000x

www.rsc.org/

A new amphiphilic boron-dipyrromethene (BODIPY) dye **1** with a hydrophobic wedge at the *meso*-position and two hydrophilic cationic moieties at boron was synthesized. Temperature- and concentration-dependent UV/Vis spectroscopic studies in water were conducted to explore the self-assembly process of the dye. Detailed analysis of the data using two different models (developed by Van der Schoot et al. and Goldstein et al. respectively) for cooperative supramolecular polymerization indicates distinctly a nucleation-growth mechanism of the aggregation of dye **1** and the nucleus size (ca. 12-18 molecules) and cooperativity factor (ca. 0.01) could be derived. Further investigation by transmission electron microscopy, scanning confocal microscopy, and X-ray diffraction revealed a unique vesicular morphology of the aggregates with multilamellar wall structure. Meanwhile, these dye vesicles exhibit unique optical characteristics, *i.e.* red-shifted sharp absorption band, narrowed emission linewidth, and increase in fluorescence quantum yield, as compared with the monomeric dye.

Introduction

The self-assembly of chromophoric amphiphiles has been impressively demonstrated as an effective strategy for generating highly ordered nanostructures with outstanding functions.¹ A large number of π -conjugated chromophores, such as carbocyanines,² porphyrins,³ naphthalene/perylene dimides,⁴ oligo(*p*-phenylene)s,⁵ oligo(*p*-phenylenevinylene)s,⁶ fullerenes,⁷ and hexabenzocoronenes,⁸ have been chemically modified to be amphiphilic building blocks for self-assembly in aqueous media. By fine tuning the structures of hydrophobic and hydrophilic segments of these molecular building blocks, a variety of functional supramolecular aggregates including nanotubes,^{2,4e,8} nanorods,^{3d} vesicles,^{3a-c,4a-c,6,7} micellar particles,^{4d,5} as well as nanofibers,⁵ have been constructed.

Boron-dipyrromethene (BODIPY) dyes belong to the most interesting functional dyes⁹ and have been widely applied for biolabeling,¹⁰ fluorescent sensing and imaging,¹¹ dye lasers,¹² as well as photovoltaics,¹³ owing to their outstanding optical and electronic properties. The supramolecular assemblies of BODIPYs including organogels,¹⁴ columnar stacks,¹⁵ electrostatic complex,¹⁶ in organic solvents or liquid crystalline states have been investigated. More recently, the formation of H-type extended aggregates¹⁷ and emissive nanoparticles¹⁸ have been reported for amphiphilic BODIPYs. Nevertheless, the studies on aqueous self-assembly behaviour of this class of dyes remain less and there is still a lack of detailed understanding of the mechanistic and thermodynamic aspects

of the self-assembly process for BODIPY dyes in aqueous media, which is crucial for rational control of the spatial organization of the stacked dye molecules and the relevant functional properties. Generally, highly ordered structures can be produced via a cooperative nucleation-growth pathway¹⁹ while an isodesmic process²⁰ (same equilibrium constant for all binding events) leads to less organized assemblies with lack of internal order.²¹ For the self-assembly of a neutral amphiphilic BODIPY dye in water, the isodesmic mechanism has been reported.¹⁷ In contrast, the aggregation mechanism of charged BODIPY amphiphiles remains unexplored.

To address the above-mentioned consideration, we have designed and synthesized a new amphiphilic BODIPY dye **1** by introducing two hydrophilic substituents with cationic quaternary ammonium groups at the boron and a hydrophobic 3,4,5-tris(*n*-dodecyloxy)phenyl wedge at the *meso*-position (Fig. 1). One characteristic feature of **1** is that the *meso*-phenyl ring and two boron-substituents adopt nearly orthogonal planes with respect to the dipyrromethene core, as evidenced by the crystallographic data of relevant BODIPYs.²² Such steric structure hinders the otherwise common isodesmic face-to-face stacking and may direct a highly slipped molecular arrangement which is governed by the electrostatic, π - π , and hydrophobic interactions of **1**. To gain structural and mechanistic details of the self-assembly of dye **1** in water, spectroscopic and microscopic methods were applied for investigation.

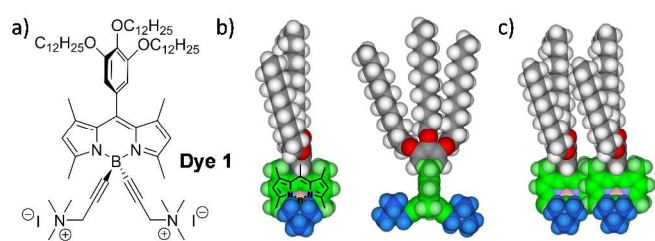
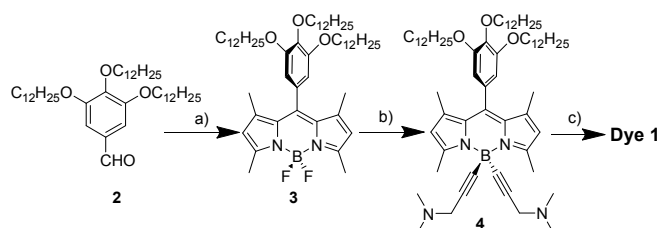


Fig. 1 a) Chemical structure of dye **1**. b) Front and side views of the space-filling (CPK) model of **1**. The dipyrromethene core and the hydrophilic groups were illustrated in green and blue color, respectively. c) Schematic representation of the slipped packing of two molecules of **1**.

Results and Discussion

The amphiphilic dye **1** was synthesized starting from the condensation of 3,4,5-tridodecyloxybenzaldehyde **2** and 2,4-dimethylpyrrole (Scheme 1). The intermediate BF₂-dipyrromethene **3** was reacted with the Grignard reagent of 1-dimethylamino-2-propyne to give the boron-substituted dye **4**. Subsequent methylation of the amino groups of **4** with methyl iodide afforded the targeted compound **1**. The dye **1** was fully characterized by NMR, MS, elemental analysis, and optical spectroscopy (see ESI). In polar organic solvent DMSO, a UV/Vis absorption spectrum typical for molecular dissolved BODIPYs²³ was observed for **1** with a S₀-S₁ absorption band between 450 and 525 nm ($\lambda_{\text{max}} = 500$ nm). The corresponding emission spectrum ($\lambda_{\text{max}} = 512$ nm) is approximately a mirror image of the S₀-S₁ absorption band and the fluorescence quantum yield was measured as 17% in DMSO.



Scheme 1 Synthesis of dye **1**. Reagents and conditions: a) 2,4-dimethylpyrrole, CF₃COOH, CH₂Cl₂, DDQ, r.t., 2 h, then BF₃•Et₂O, triethylamine, r.t., 10 h, 30% over all; b) 1-dimethylamino-2-propyne, EtMgBr, THF, 60 °C, 12 h, 75%; c) CH₃I, diethyl ether, 30 °C, 24 h, 94%.

Despite its large sized hydrophobic wedge, the amphiphilic dye **1** was found to be soluble in water. At a low concentration of 2.0×10^{-7} M, a UV/Vis absorption spectrum of monomeric **1** was observed (Fig. 2), which displays a S₀-S₁ absorption band between 425 and 550 nm ($\lambda_{\text{max}} = 509$ nm) with a vibronic sub-band at around 470 nm. The corresponding emission band is located at $\lambda_{\text{max}} = 523$ nm. In contrast to the spectra for the monomeric dye, remarkable spectral changes were observed for dye **1** at a higher concentration of 1.0×10^{-5} M. A narrow, bathochromically-shifted band (J-band) and a structured, hypsochromically-shifted band (H-band) appeared at $\lambda_{\text{max}} = 529$ nm and $\lambda_{\text{max}} = 480$ nm, respectively, indicating unambiguously the formation of dye **1** aggregates.

The emission spectrum of the dye aggregates is much narrower than that of the monomers and displays a mirror-image relationship to the J-band with a small Stokes shift of 3 nm. For the monomeric dye **1**, $\Phi_{\text{mon}} = 0.5\%$ was measured in water (2.0×10^{-7} M), whereas a measurable increase in the fluorescence quantum yield was observed upon increasing concentration of dye **1**. At a concentration of 1.0×10^{-5} M, a fluorescence quantum yield $\Phi_{\text{agg}} = 2.2\%$ was obtained for the aggregates, which is about 4 times of that of monomeric **1**. The increase in the fluorescence quantum yield upon aggregation may be explained in terms of aggregation-induced emission enhancement.^{18b,c} The fluorescence excitation spectrum for the dye aggregates (Fig. S6†) strongly resembles the absorption profile, confirming that the H-band and J-band originate from the same aggregated species. Furthermore, a fluorescence lifetime of 0.3 ns was observed for the aggregates of dye **1** (Fig. S7†), which is much shorter than that of the monomers (2.5 ns). The observed significantly narrowed absorption and emission bands, small Stokes shift, and decrease in fluorescence lifetime for the dye **1** aggregates with respect to those of monomers are highly characteristic for J-aggregates.²⁴

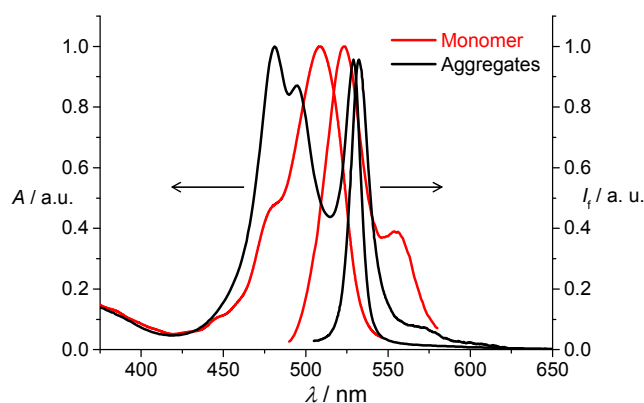


Fig. 2 UV/Vis absorption and fluorescence spectra of dye **1** in water at concentrations of 2.0×10^{-7} M (red, $\lambda_{\text{ex}} = 470$ nm) and 1.0×10^{-5} M (black, $\lambda_{\text{ex}} = 470$ nm).

The aggregation process of dye **1** in water was further monitored by temperature- and concentration-dependent UV/Vis absorption spectroscopy (Fig. 3 and Fig. S8†). Upon progressively increasing the temperature, a gradual increase in the monomer band and a concomitant decrease in the H- and J-bands were observed for dye **1** at a concentration of 1.0×10^{-5} M. Plotting the apparent absorption coefficients of the monomer and aggregate bands versus temperature yields sigmoidal type curves (Fig. 3a). However, when the spectral data was analysed by applying isodesmic (equal-K) model,²⁰ significant deviation of the experimental data points from the theoretical curve can be observed (Fig. 3b). Thus, the experimental data displays a much sharper monomer-aggregate transition around 320 K in comparison with the isodesmic curve, implying a highly cooperative self-assembly process of dye **1**. This was confirmed when the nucleation-growth model

developed by Meijer, Schenning, and Van der Schoot was used for data evaluation.¹⁹ In this model, a step of formation of critical-sized nucleus is considered before the subsequent propagation steps. Applying this model, an obvious improvement of the data fitting was observed and an elongation temperature $T_e = 317$ K was given at the concentration of 1.0×10^{-5} M. For the nucleation regime of this model, a small dimensionless constant $K_a = (4 \pm 2) \times 10^{-4}$ was obtained, confirming a high degree of cooperativity of the self-assembly of dye **1**. Based on the K_a value, the average size of nuclei for initiating elongation at T_e is given by $1/K_a^{1/3}$. For dye **1**, a relatively large nuclei size of 12-18 molecules was obtained.

Goldstein and Stryer's model and the fitting of experimental data of dye **1** at 509 nm (circles) from concentration-dependent UV/Vis absorption spectra (see ESI) to the curve with $s = 15$ and $\sigma = 0.015$.

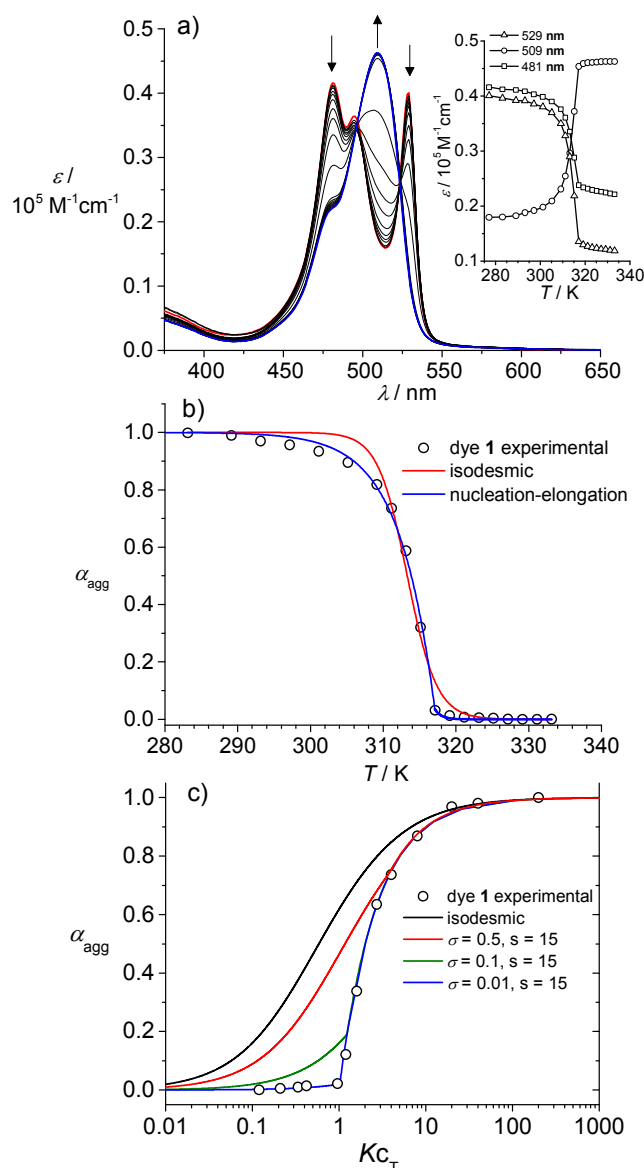


Fig. 3 (a) Temperature-dependent UV/Vis absorption spectra of dye **1** at a concentration of 1.0×10^{-5} M in water from 4 °C (red) to 60 °C (blue). The arrows indicate the spectra changes with increasing temperature. Inset: Plot of the apparent absorption coefficients at 529, 509, and 481 nm versus temperature. (b) Plot of fraction of aggregated molecules α_{agg} at 509 nm (circles) as a function of temperature and the fitting curves with isodesmic model and nucleation-growth model. (c) Plot of α_{agg} versus Kc_T with various s and σ values according to

The cooperativity of the self-assembly process of dye **1** was further verified by concentration-dependent UV/Vis spectroscopic studies (Fig. S8†). The observed spectral changes upon concentration variation are highly comparable with those in temperature-dependent measurements. In agreement with the temperature-dependent studies, the aggregation behavior of dye **1** cannot be well described by the isodesmic model, as shown by nonlinear least-square regression analysis of the concentration-dependent UV/Vis spectral data (Fig. 3c). The spectra data was further evaluated with the cooperative model purposed by Goldstein and Stryer.²⁵ Based on this model, a nucleus of size s is formed through a isodesmic process with an equilibrium constant K_s while further aggregation takes place with equal equilibrium constant K ($K > K_s$), i.e. $K_1 = K_2 = \dots = K_s$ and $K_{s+1} = K_{s+2} = \dots = K$. The cooperativity is reflected by the parameter σ defined as $\sigma = K_s/K$. For a highly cooperative aggregation, $\sigma \ll 1$ is expected. Recently, this model has been successfully used for the study of cooperative self-assembly process of bis(merocyanine) dyes.²⁶ As depicted in Fig. 3c, the obtained experimental data points for dye **1** in water could be manually fitted to the calculated curves and the best data fitting was obtained for a σ value of 0.01 with an equilibrium constant $K = (4.0 \pm 0.1) \times 10^5 \text{ M}^{-1}$, indicating a highly cooperative process of this dye. The critical concentration for aggregation is around 2.5×10^{-6} M. The nucleus size could be estimated as 10-20 molecules, which are in agreement with that obtained from temperature-dependent studies. It is worth to note that with a σ value of 0.01, the difference of curves for nucleus size s of 10-20 are significantly small and the exact value of s is unable to be obtained in this case.

The formation of J-aggregates of dye **1** can also be mediated by solvent variation. In “good solvent” such as DMSO, the UV/Vis absorption spectrum of BODIPY **1** displayed a molecular dissolved absorption band between 450 and 525 nm for the S_0 - S_1 transition with $\lambda_{\text{max}} = 500$ nm. Upon addition of water into the DMSO solution of dye **1**, a gradual decrease of the monomer band and rise of both J-band and H-band was observed, indicating the transition from monomers to dye aggregates (Fig. S9†). The aggregation process in DMSO/water was further monitored by ^1H NMR spectroscopy. The spectra of non-aggregated dye **1** displays sharp and well-resolved signals of H_a and H_b in deuterated DMSO (Fig. 4) at $\delta = 6.58$ ppm and $\delta = 6.28$ ppm, respectively. Upon addition of D_2O , the signals of the protons of H_a and H_b are dramatically shifted to upfield with significantly broadening of the signals, implying the formation of aggregates of dye **1**. At a D_2O content of 90%, the peaks of H_a and H_b are shifted respectively to 6.17 and 5.90 ppm. The upfield shift of protons is consistent with magnetic shielding effect of the π -electrons of neighbouring dye molecules that are stacked closely.

For the amphiphilic dye **1**, the morphology of aggregates could be roughly estimated from Israelachvili's critical packing

parameter P_c (or shape factor).²⁷ For dye **1**, $P_c \approx 0.8$ was calculated (see ESI), implying the formation of vesicular aggregates should be favoured in water.²⁸ To verify the prediction, drop-cast samples of the dye **1** aggregates in water were prepared on a formvar/carbon coated grid and visualized by transmission electron microscopy (TEM). In contrast with the well-known tubular morphology of the J-aggregates of amphiphilic cyanine dyes ($P_c \approx 0.5$),²⁹ hollow spherical vesicular aggregates were observed for the amphiphilic BODIPY dye **1**. The vesicular morphology is in agreement with that predicted by Fig. 5a shows vesicular aggregates of dye **1** with diameters of 100-160 nm. The wall thickness of the vesicles is uniform and about 20 nm, which is approximately 8 times the length of a single dye molecule (about 2.5 nm obtained from molecular modelling for stretched alkyl chains), suggesting a multiple-layered structure of the vesicles. The average size and wall thickness of the vesicular aggregates are affected by preparation method. If the aggregates were prepared by "solvent switch" method³⁰ in DMSO-containing water (0.5% DMSO, v/v), vesicular aggregates with smaller size and thinner wall than those prepared by organic-solvent-free method were observed (Fig. S10†).

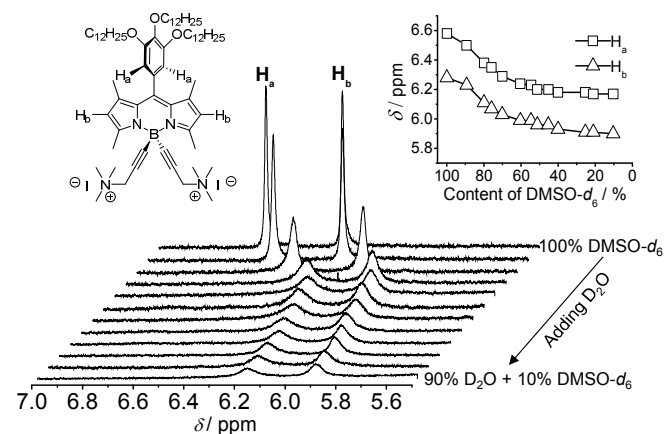


Fig. 4 ^1H NMR spectra of **1** self-assembly in $\text{D}_2\text{O}/\text{DMSO}-d_6$ (10 mg/mL) with D_2O content from 10% to 100%.

The vesicular nature of these dye aggregates was confirmed by further small-angle X-ray diffraction (SAXD) measurements (Fig. 5b). For a bulk sample of **1**, a strong reflection at $q = 1.28 \text{ nm}^{-1}$ was observed ($q = 4\pi\sin\theta/\lambda$, where λ is the X-ray wavelength and 2θ the scattering angle). In addition, two relatively weak reflections at 2.55 and 3.89 nm^{-1} were resolved. The three reflections have a q -ratio of 1:2:3 with satisfactory accuracy, which can be indexed as the (001), (002), and (003) reflections of the multilamellar structure of **1**. For the aggregates in water, the (001) reflection can be observed at $q = 1.32 \text{ nm}^{-1}$. In both cases, the (001) reflection indicate a repeat spacing of the lamellar bilayers about 4.8 nm , approximately twice of the length of dye **1** molecule. Owing to their J-aggregation properties, the large-sized vesicles of **1** are fluorescent and can be observed under scanning confocal microscope (Fig. 5c-h). The images of serial slices made along

the z -direction of a single vesicle revealed a transition from a solid spot to a ring, then again to a solid spot, demonstrating the hollow vesicular structure. The emission spectra collected by confocal scanning of the sample (Fig. 5i, $\lambda_{\text{exc}} = 488 \text{ nm}$) are in excellent agreement with that obtained by conventional spectrometer, confirming the formation of fluorescent vesicular aggregates of dye **1**.

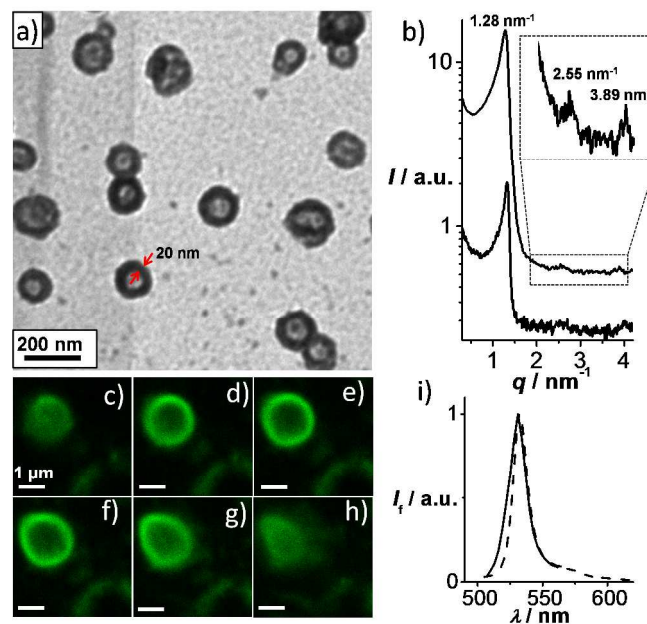


Fig. 5 (a) TEM image of the vesicular aggregates of dye **1** in water (0.1 mg/mL). (b) Small angle X-ray diffraction (SAXD) pattern for dye **1** in bulk (top) and in water (bottom). (c)-(h) Z-scan confocal microscopic images of a single vesicles of dye **1**, scale bar: $1 \mu\text{m}$. i) The fluorescence profile of the dye aggregates collected by confocal microscope (solid line, $\lambda_{\text{exc}} = 488 \text{ nm}$) and conventional fluorescence spectrometer (dashed line, $\lambda_{\text{ex}} = 470 \text{ nm}$).

In such vesicular aggregates, a highly slipped J-type arrangement of the dipyrromethene units could be directed by the steric boron-substituents and the *meso*-phenyl ring (Fig. 6). Accordingly, the chromophores are slip-stacked with their S_0 - S_1 transition dipoles tangentially aligned with respect to the surface curvature of the vesicles. For the stability of this molecular packing in water, it is important that the hydrophilic cationic groups of **1** are exposed to water while the hydrophobic alkyl chains are packed together to form bilayers and minimise the free energy. The cooperative self-assembly of dye **1** is driven by intermolecular attractive forces including hydrophobic effect and π - π interaction, which are balanced with the repulsive electrostatic interaction of the cationic head groups.

The molecular arrangement of dye **1** within the layer could be further evaluated if the observed absorption properties were rationalized with molecular exciton theory.³¹ According to this theory, the H- and J-bands for dye **1** aggregates could be identified as components of Davydov-split transitions arising from a 2D herringbone-type molecular arrangement, as reported for the J-aggregates of several carbocyanine dyes.³² By assuming a molecular arrangement with two translationally

non-equivalent molecules in one unit cell, the tilt angle α of the slipped stacking of **1** can be simply estimated by the relationship $(f_H/\bar{\nu}_H) / (f_J/\bar{\nu}_J) = \text{ctg}2\alpha$,^{32b-d} where f_H and f_J are the oscillator strength for the H- and J-bands, respectively, and $\bar{\nu}_H$ and $\bar{\nu}_J$ are the corresponding transition energies. From the UV/Vis absorption spectrum for the aggregates of dye **1**, $\alpha \approx 30^\circ$ was estimated, as shown in the packing model of the vesicular aggregates of dye **1** (Fig. 6).

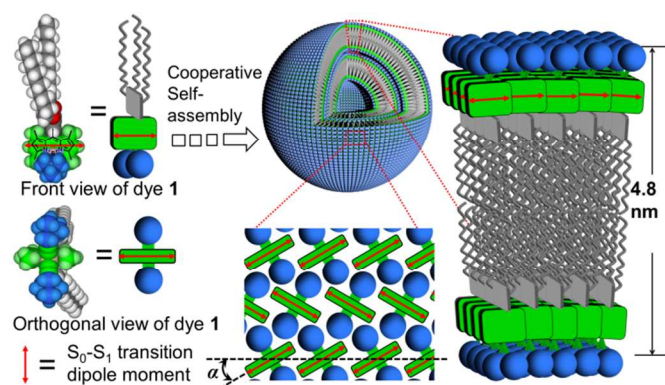


Fig. 6 Schematic illustration of putative molecular packing for the vesicular aggregates of dye **1**. The dipyrromethene core and the hydrophilic groups of **1** were illustrated in green and blue colour, respectively. The red arrows indicate the S_0-S_1 transition dipole moments of **1**.

Conclusions

In summary, a new amphiphilic boron-substituted BODIPY dye has been synthesized by attaching cationic hydrophilic substituents at boron atom and hydrophobic alkyl chains at the *meso*-phenyl group. This functional dye self-assembles into fluorescent vesicular aggregates in water through a highly cooperative self-assembly process. In contrast with the isodesmic mechanism for the extended aggregates of the reported nonpolar and neutral amphiphilic BODIPY dyes,^{15,17} a nucleation-growth mechanism for the formation of vesicular aggregates of a charged BODIPY amphiphiles was demonstrated for the first time according to the Meijer-Schenning-Van-der-Schoot model and the Goldstein-Stryer model for cooperative supramolecular polymerization, indicating the hydrophobic as well as electrostatic interactions are important source of cooperativity. The parameters including nucleus size of ca. 12-18 molecules and cooperativity factor of ca. 0.01 have been derived for the aggregation process. Furthermore, the BODIPY vesicular assemblies display optical characteristics comparable with those of the classical cyanine dye based J-aggregates, which could be attribute to a highly slipped 2D herringbone-type packing directed by the steric and amphiphilic feature of the dye. With their unique hollow vesicular morphology and optical properties, the BODIPY J-aggregates may have the potential to be further functionalized by the loading of guest molecules toward applications in artificial light harvesting and fluorescence sensing.

Acknowledgements

This work is supported by the National Natural Science Foundation of China (No. 21176184, No. 21304069), Program for New Century Excellent Talents by the Ministry of Education (NCET-09-0584).

Notes and references

^aSchool of Chemical Engineering and Technology, and Collaborative Innovation Center of Chemical Science and Chemical Engineering (Tianjin), Tianjin University, Tianjin, 300072, China. Fax: (+86)22-27374971; E-mail: zjchen@tju.edu.cn

^bKey Laboratory of Advanced Materials, School of Material Science & Engineering, Tsinghua University, Beijing, 100084, China

[†]Electronic supplementary information (ESI) available: Experimental and spectral data, TEM image.

- (a) D. Görl, X. Zhang and F. Würthner, *Angew. Chem. Int. Ed.*, 2012, **51**, 6328; (b) S. S. Babu, V. K. Praveen and A. Ajayaghosh, *Chem. Rev.*, 2014, **114**, 173; (c) M. R. Molla and S. Ghosh, *Phys. Chem. Chem. Phys.*, 2014, **16**, 26672; (d) C. Wang, Z. Wang, and X. Zhang, *Acc. Chem. Res.*, 2012, **45**, 608; (e) J. -H. Ryu, D. -K. Hong and M. Lee, *Chem. Commun.*, 2008, **44**, 1042; (f) F. J. M. Hoeben, P. Jonkheijm, E. W. Meijer and A. P. H. J. Schenning, *Chem. Rev.*, 2005, **105**, 1491.
- (a) D. M. Eisele, C. W. Cone, E. A. Bloemsma, S. M. Vlaming, C. G. F. van der Kwaak, R. J. Silbey, M. G. Bawendi, J. Knoester, J. P. Rabe and D. A. Vanden Bout, *Nat. Chem.*, 2012, **4**, 655; (b) D. M. Eisele, J. Knoester, S. Kirstein, J. P. Rabe and D. A. Vanden Bout, *Nat. Nanotechnol.*, 2009, **4**, 658.
- (a) F. J. Lovell, S. C. Jin, E. Huynh, H. Jin, C. Kim, L. J. Rubinstein, C. W. W. Chan, W. Cao, V. L. Wang and G. Zheng, *Nat. Mat.*, 2011, **10**, 324; (b) Y. Li, X. Li, Y. Li, H. Liu, S. Wang, H. Gan, J. Li, N. Wang, X. He and D. Zhu, *Angew. Chem. Int. Ed.*, 2006, **45**, 3639; (c) T. Komatsu, E. Tsuchida, C. Böttcher, D. Donner, C. Messerschmidt, U. Siggel, W. Stocker, P. J. Rabe and J. H. Fuhrhop, *J. Am. Chem. Soc.*, 1997, **119**, 11660; (d) A. D. Schwab, D. E. Smith, C. S. Rich, E. R. Young, W. F. Smith and de Paula J. C., *J. Phys. Chem. B*, 2003, **107**, 11339.
- (a) X. Zhang, Z. Chen and F. Würthner, *J. Am. Chem. Soc.* 2007, **129**, 4886; (b) X. Zhang, S. Rehm, M. M. Safont-Sempere and F. Würthner, *Nat. Chem.*, 2009, **1**, 623. (c) M. R. Molla and S. Ghosh, *Chem. Eur. J.*, 2012, **18**, 9860; (d) M. Kumar and S. J. George, *Chem. Eur. J.*, 2011, **17**, 11102; (e) H. Shao, M. Gao, S. E. Kim, C. P. Jaroniec and J. R. Parquette, *Chem. Eur. J.*, 2011, **17**, 12882; (f) D. Ke, C. Zhan, S. Xu, X. Ding, A. Peng, J. Sun, S. He, A. D. Q. Li and J. Yao, *J. Am. Chem. Soc.*, 2011, **133**, 11022.
- J. -H. Ryu, E. Lee, Y. -b. Lim and M. Lee, *J. Am. Chem. Soc.*, 2007, **129**, 4808.
- J. M. F. Hoeben, O. I. Shklyarevskiy, J. M. Pouderoijen, H. Engelkamp, P. H. J. A. Schenning, C. M. P. Christianen, C. J. Maan and E. W. Meijer, *Angew. Chem. Int. Ed.*, 2006, **45**, 1232.
- (a) M. Sano, K. Oishi, T. Ishi-i and S. Shinkai, *Langmuir*, 2000, **16**, 3773; (b) Y. Zhao and G. Chen, *Struct. Bond*, 2014, **159**, 23.
- (a) W. Zhang, W. Jin, T. Fukushima, A. Saeki, S. Seki and T. Aida, *Science*, 2011, **334**, 340; (b) J. P. Hill, W. Jin, A. Kosaka, T.

- Fukushima, H. Ichihara, T. Shimomura, K. Ito, T. Hashizume, N. Ishii and T. Aida, *Science*, 2004, **304**, 1481.
- 9 For reviews, see (a) A. Loudet, K. Burgess, *Chem. Rev.*, 2007, **107**, 4891; (b) G. Ulrich, R. Ziessel and A. Harriman, *Angew. Chem. Int. Ed.* 2008, **47**, 1184; (c) G. Fan, L. Yang and Z. Chen, *Front. Chem. Sci. Eng.*, 2014, **8**, 405.
- 10 (a) L. Li, J. Y. Han and K. Burgess, *J. Org. Chem.*, 2008, **73**, 1963; (b) S. Niu, C. Massif, G. Ulrich, P.-Y. Renard, A. Romieu and R. Ziessel, *Chem. Eur. J.* 2012, **18**, 7229.
- 11 (a) N. Boens, V. Leen and W. Dehaen, *Chem. Soc. Rev.*, 2012, **41**, 1130; (b) J. Fan, M. Hu, P. Zhan and X. Peng, *Chem. Soc. Rev.*, 2013, **42**, 29.
- 12 O. García, R. Sastre, D. d. Agua, A. Costela, I. García-Moreno, F. López Arbeloa, J. B. Prieto and I. L. Arbeloa, *J. Phys. Chem. C*, 2007, **111**, 1508.
- 13 (a) B. Kim, B. Ma, V. R. Donuru, H. Liu and J. M. J. Fréchet, *Chem. Commun.*, 2010, **46**, 4148; (b) T. Bura, N. Leclerc, S. Fall, P. Lévesque, T. Heiser, P. Retailleau, S. Rihn, A. Mirloup and R. Ziessel, *J. Am. Chem. Soc.*, 2012, **134**, 17404; (c) T. Rousseau, A. Cravino, T. Bura, G. Ulrich, R. Ziessel and J. Roncali, *Chem. Commun.*, 2009, **45**, 1673; (d) Q.-C. Yu, W.-F. Fu, J.-H. Wan, X.-F. Wu, M.-M. Shi and H.-Z. Chen, *ACS Appl. Mater. Interfaces*, 2014, **6**, 22496.
- 14 F. Camerel, L. Bonardi, M. Schmutz and R. Ziessel, *J. Am. Chem. Soc.*, 2006, **128**, 4548-4549.
- 15 A. Florian, M. J. Mayoral, V. Stepanenko and G. Fernández, *Chem. Eur. J.*, 2012, **18**, 14957.
- 16 J. Barberá, E. Bahaidarah, A. Harriman and R. Ziessel, *J. Am. Chem. Soc.*, 2012, **134**, 6100.
- 17 N. K. Allampally, A. Florian, M. Mayoral, C. Rest, V. Stepanenko and G. Fernández, *Chem. Eur. J.*, 2014, **20**, 10669.
- 18 (a) J.-H. Olivier, J. Widmaier and R. Ziessel, *Chem. Eur. J.*, 2011, **17**, 11709; (b) S. Choi, J. Bouffard and Y. Kim, *Chem. Sci.*, 2014, **5**, 751; (c) M. Baglan, S. Ozturk, B. Gür, K. Meral, U. Bozkaya, O. A. Bozdemir and S. Atilgan, *RSC Adv.*, 2013, **3**, 15866.
- 19 (a) P. Jonkheijm, P. Van der Schoot, A. P. H. J. Schenning and E. W. Meijer, *Science*, 2006, **313**, 80; (b) T. F. A. De Greef, M. M. J. Smulders, M. Wolffs, A. P. H. J. Schenning, R. P. Sijbesma and E. W. Meijer, *Chem. Rev.*, 2009, **109**, 5687; (c) D. Zhao and J. S. Moore, *Org. Biomol. Chem.*, 2003, **1**, 3471.
- 20 (a) R. B. Martin, *Chem. Rev.*, 1996, **96**, 3043; (b) Z. Chen, A. Lohr, C. R. Saha-Möller and F. Würthner, *Chem. Soc. Rev.*, 2009, **38**, 564.
- 21 (a) C. Kulkarni, S. Balasubramanian and S. George, *ChemPhysChem*, 2013, **14**, 661; (b) T. Rudolph, N. K. Allampally, G. Fernández and F. H. Schacher, *Chem. Eur. J.*, 2014, **20**, 13871.
- 22 (a) Y. Chen, L. Wan, D. Zhang, Y. Bian and J. Jiang, *Photochem. Photobiol. Sci.*, 2011, **10**, 1030; (b) C. Goze, G. Ulrich and R. Ziessel, *Org. Lett.*, 2006, **8**, 4445.
- 23 F. Bergström, I. Mikhalyov, P. Häggglöf, R. Wortmann, T. Ny and L. B.-Å. Johansson, *J. Am. Chem. Soc.*, 2002, **124**, 196.
- 24 (a) F. Würthner, T. E. Kaiser and C. R. Saha-Möller, *Angew. Chem. Int. Ed.*, 2011, **50**, 3376; (b) *J-Aggregates*, ed. T. Kobayashi, World Scientific, Singapore, 2012, vol. 2.
- 25 R. F. Goldstein and L. Stryer, *Biophys. J.*, 1986, **50**, 583.
- 26 G. Fernández, M. Stolte, V. Stepanenko, and F. Würthner, *Chem. Eur. J.*, 2013, **19**, 206.
- 27 J. Israelachvili, *Colloids Surf. A*, 1994, **91**, 1.
- 28 T. Shimizu, M. Masuda and H. Minamikawa, *Chem. Rev.*, 2005, **105**, 1401.
- 29 S. Kirstein and S. Dähne, *Int. J. Photoenergy*, 2006, **5**, 1.
- 30 J. Du and R. K. O'Reilly, *Soft Mater*, 2009, **5**, 3544.
- 31 (a) M. Kasha, H. R. Rawls and M. A. El-Bayoumi, *Pure Appl. Chem.*, 1965, **11**, 371; (b) A. S. Davydov, *Theory of molecular excitons*, Plenum Press, New York, 1971.
- 32 (a) S. Kirstein, R. Steitz, R. Garbella and H. Möhwald, *J. Chem. Phys.*, 1995, **103**, 818; (b) S. Kirstein and H. Möhwald, *J. Chem. Phys.*, 1995, **103**, 826; (c) M. L. Dekhtyar' and V. M. Rozenbaum, *J. Struct. Chem.*, 1995, **3**, 167; (d) V. N. Bumyuk, S. Kirstein and H. Möhwald, *J. Phys. Chem.*, 1993, **97**, 569; (e) H. v. Berlepsch and C. Böttcher, *Langmuir*, 2013, **29**, 4948.